

Journal of Biomedical Optics

BiomedicalOptics.SPIEDigitalLibrary.org

Assessing the sensitivity of human skin hyperspectral responses to increasing anemia severity levels

Gladimir V. G. Baranoski
Ankita Dey
Tenn F. Chen

Assessing the sensitivity of human skin hyperspectral responses to increasing anemia severity levels

Gladimir V. G. Baranoski,* Ankita Dey, and Tenn F. Chen

University of Waterloo, Natural Phenomena Simulation Group, School of Computer Science, 200 University Avenue, Waterloo, Ontario N2L 3G1, Canada

Abstract. Anemia is a prevalent medical condition that seriously affects millions of people all over the world. In many regions, not only its initial detection but also its monitoring are hindered by limited access to laboratory facilities. This situation has motivated the development of a wide range of optical devices and procedures to assist physicians in these tasks. Although noticeable progress has been achieved in this area, the search for reliable, low-cost, and risk-free solutions still continues, and the strengthening of the knowledge base about this disorder and its effects is essential for the success of these initiatives. We contribute to these efforts by closely examining the sensitivity of human skin hyperspectral responses (within and outside the visible region of the light spectrum) to reduced hemoglobin concentrations associated with increasing anemia severity levels. This investigation, which involves skin specimens with distinct biophysical and morphological characteristics, is supported by controlled *in silico* experiments performed using a predictive light transport model and measured data reported in the biomedical literature. We also propose a noninvasive procedure to be employed in the monitoring of this condition at the point-of-care. © The Authors. Published by SPIE under a Creative Commons Attribution 3.0 Unported License. Distribution or reproduction of this work in whole or in part requires full attribution of the original publication, including its DOI. [DOI: [10.1117/1.JBO.20.9.095002](https://doi.org/10.1117/1.JBO.20.9.095002)]

Keywords: anemia; skin reflectance; optical monitoring; simulation.

Paper 150320R received May 12, 2015; accepted for publication Jul. 27, 2015; published online Sep. 3, 2015.

1 Introduction

Although recent advances in optical technologies are enabling remarkable improvements in the prevention and timely treatment of a wide range of diseases, there are still many challenges ahead, notably involving primary health care for populations that rely on low-resources diagnosis settings. Among these challenges, one can highlight the development of cost-effective procedures and devices for the screening and monitoring of pervasive medical conditions such as anemia, which can compromise the health of individuals of all ages, races, and ethnicities.¹ According to the World Health Organization (WHO), approximately one quarter of the human population is affected by anemia, and this medical condition represents a public health problem in both industrialized and nonindustrialized countries.^{2,3}

Anemia is a blood disorder usually associated with a decrease in the number of red blood cells (RBCs)⁴ encapsulating hemoglobin (Hb) proteins.⁴ The two functional forms of the Hb proteins, namely oxyhemoglobin (O₂Hb) and deoxyhemoglobin (HHb),⁵ correspond to the oxygenated and deoxygenated states of Hb molecules, respectively, which play a pivotal role in the maintenance of an individual's normal physiological status. While an O₂Hb molecule contains iron atoms in a ferrous state, which allows them to bind with oxygen, an HHb molecule contains iron atoms in a ferric (oxidized) state, which prevents this binding.

There are three main types of this disorder, namely iron-deficiency anemia (IDA), pernicious anemia, and hemolytic

anemia.^{1,4} These are elicited by different factors that can alter the production of healthy RBCs by the bone marrow. This complex biochemical process requires proteins, iron, vitamin B12, folate, and small amounts of other minerals and vitamins. For example, IDA, the most common type of anemia, results from a low supply of iron. According to the World Health Organization (WHO), it is one of the main factors contributing to the global burden of diseases.^{2,3} In the case of pernicious anemia, it is primarily caused by an insufficient absorption of vitamin B12. Hemolytic anemia, on the other hand, may take place when a significant number of RBCs are destroyed and removed from the bloodstream through hemolysis before the normal end of their lifespan, and the bone marrow cannot produce enough new RBCs to replace them. This type of anemia can be acquired or inherited. It is also worth mentioning that there are types of anemia, such as aplastic anemia, associated with a lower than normal presence of other blood formed elements, such as white blood cells and platelets. The study of these types of anemia, however, is beyond the scope of this work.

The investigation presented here focuses on the most common types of anemia, which can seriously impair the blood's capability of transporting oxygen from respiratory organs (lungs) to the rest of the body.⁶ This, in turn, not only compromises an individual's overall health, but may also lead to life-threatening situations.^{1,4} Although the Hb concentration in the blood alone cannot be used to diagnose anemia, it can provide useful information for determining its severity level.¹ Accordingly, several optical devices and image-based procedures have been proposed for the low-cost estimation of Hb concentration. These devices and procedures can be loosely divided into two groups: invasive and noninvasive.

*Address all correspondence to: Gladimir V. G. Baranoski, E-mail: gvgbaran@cs.uwaterloo.ca

Devices belonging to the invasive group tend to provide more accurate results since they perform *in vitro* measurements on actual blood samples.^{7,8} However, they may still be subjected to errors during the collection and chemical analysis of the samples.^{9,10} In addition, the extraction of blood samples may bring some discomfort and, like any invasive procedure, can incur additional risks for a patient.

Devices and image-based procedures belonging to the non-invasive group, on the other hand, perform *in vivo* estimations that rely on the spectral responses of human skin to variations in Hb concentration.^{11–15} Hence, their predictive capabilities depend on the correctness of the algorithms employed to derive biophysical parameters from reflectance measurements. Since these algorithms usually involve the inversion of models used to simulate the complex interactions of light with various skin tissues and constituent materials, their estimations may be biased by several factors. These include, for example, inaccuracies in the models,¹⁶ shortcomings of the formulations used in their inversion,¹⁷ and, in the case of image-based procedures, issues related to metamerism, the phenomenon whereby colors of specimens match under specified observation conditions despite differences in the specimens' spectral reflectances.^{18,19}

In general, the fidelity of the devices and procedures belonging to either group is assessed through statistical analyses of compound estimated data. These analyses, in turn, provide qualitative trends with respect to global data, which may obscure possible quantitative limitations of these devices while handling individual cases.²⁰ Furthermore, in certain instances (e.g., involving spectrophotometry-based monitoring technology, such as pulse oximeters⁹), data are collected and analyzed off-line to determine Hb concentrations using proprietary software tools whose underlying algorithms are normally not disclosed for evaluation purposes.

As outlined above, many relevant alternatives exist to assist the diagnosis of anemia, albeit no single device or procedure is superior in all cases. In order to enhance these technologies and propose new effective solutions for the screening and monitoring of this medical condition, we believe that it is necessary to examine their related theoretical and practical constraints from different perspectives. Accordingly, in this paper, we aim to contribute to these efforts by investigating these constraints using a bottom-up approach. More specifically, we initially assess the sensitivity of human skin hyperspectral responses to fluctuations in dermal Hb concentration associated with increasing anemia severity levels. These responses are sampled within and outside the visible domain, and at distinct cutaneous sites. We then demonstrate that although possible variations on skin appearance attributes (e.g., yellowness) can be interpreted as a sign of anemia onset in some patients,¹ such visual inspections can be hindered by several physiological (e.g., skin pigmentation) and technical factors (e.g., spectral power distribution of the illuminants). Alternatively, our findings indicate that it is possible to monitor distinct levels of severity of this medical condition using relatively simple noninvasive spectral measurements that are not masked by these factors.

The remainder of this paper is organized as follows. In Sec. 2, we describe our *in silico* experimental framework, including the biophysical data used to characterize the skin specimens considered in our simulations, and introduce the sensitivity measure employed in this investigation. In Sec. 3, we present our results and discuss their practical implications regarding the noninvasive monitoring of anemia. Finally, in Sec. 4, we

close the paper and outline directions for future research in this area.

2 Materials and Methods

2.1 Simulation Framework Overview

Computer simulations,^{17,21–23} or *in silico* experiments,²⁴ are routinely being employed to accelerate the different cycles of biomedical research involving optical processes that cannot be fully studied through traditional laboratory procedures due to logistic limitations. Among these limitations, one can highlight the difficulties of performing *in vivo* measurements, notably requiring a wide variety of human tissues that may not be available in the first place, as well as the large number of biophysical variables and measurement parameters that need to be controlled during actual experiments. In order to overcome these limitations, the investigation presented in this paper is also supported by controlled *in silico* experiments. These are performed using a recently developed hyperspectral light transport model for human skin, henceforth referred to as Hyperspectral Light Impingement on Skin (HyLloS).²⁵

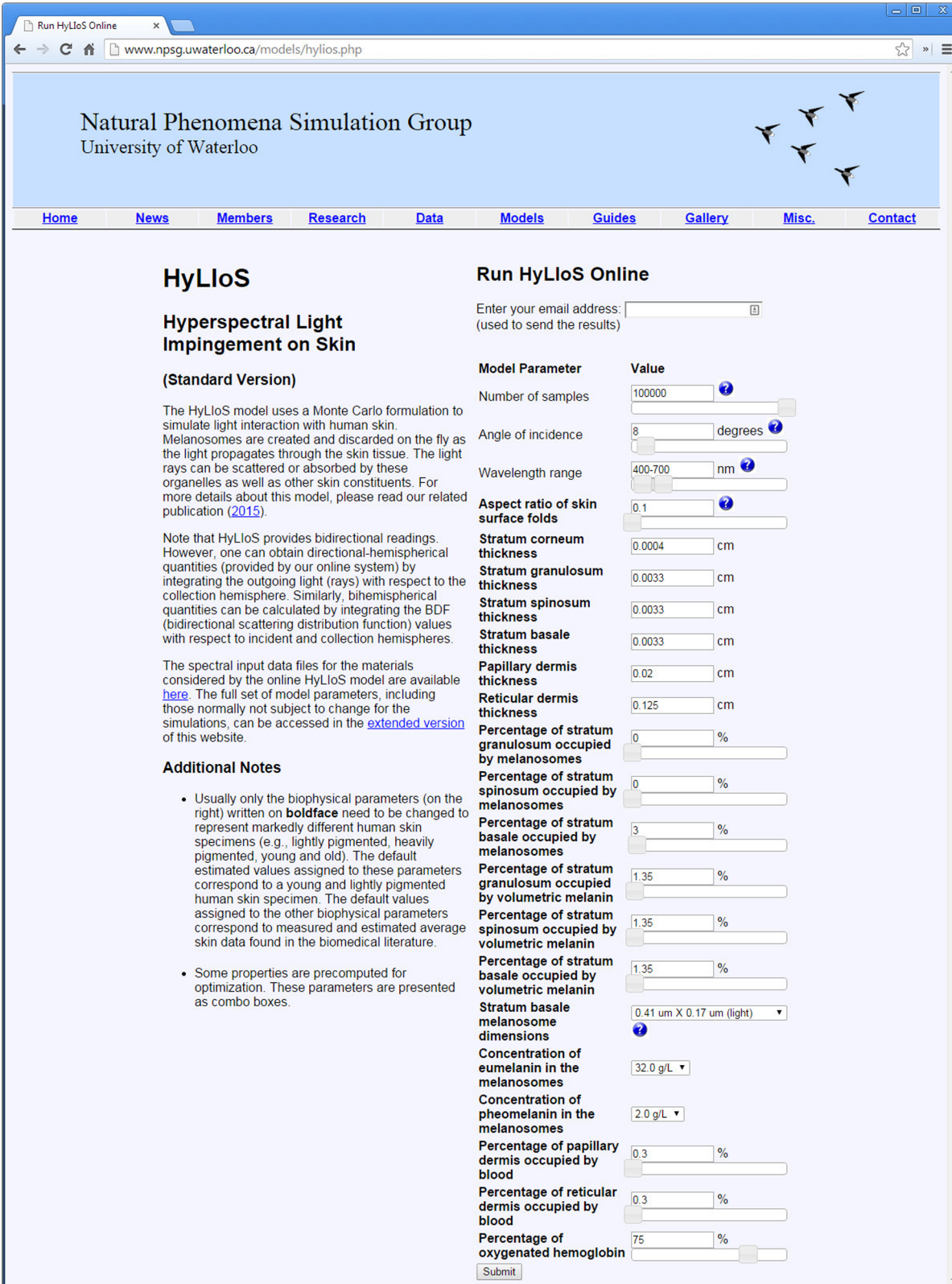
This model, capable of predictively simulating both the spectral and spatial distributions of light interacting with the skin tissues, takes into account the detailed layered structure of these tissues and the particle nature of their main light attenuation agents, namely the melanosomes, the organelles encapsulating melanin in an aggregated form.²⁶ In fact, it employs a first principles simulation approach that incorporates all main light absorbers (keratin, DNA, uranic acid, melanins, hemoglobins, beta-carotene, bilirubin, lipids, and water) and scatterers (cells, collagen fibers, melanosomes, and melanosome complexes) acting within the skin tissues in the ultraviolet (UV) (250 to 400 nm), visible (400 to 700 nm), and near-infrared (NIR) (700 to 2500 nm) domains.

Within the HyLloS algorithmic ray optics formulation, a ray interacting with a given skin specimen can be associated with any selected wavelength within the spectral regions of interest. Hence, HyLloS can provide reflectance readings with different spectral resolutions. For consistency, however, we considered a spectral resolution of 5 nm in all modeled curves depicted in this work. In terms of illumination and collection geometries, the HyLloS model can provide bidirectional reflectance quantities by recording the direction of the outgoing rays using a virtual gonireflectometer.²⁷ In addition, one can obtain directional-hemispherical reflectance quantities by integrating the outgoing rays with respect to the collection hemisphere using a virtual spectrophotometer.²⁸

To enable the full reproduction of our investigation results, we made HyLloS available online²⁹ via a model distribution system³⁰ along with the supporting biophysical data (e.g., refractive indices and extinction coefficients) used in our *in silico* experiments. This framework enables researchers to specify experimental conditions (e.g., angle of incidence and spectral range) and specimen characterization parameters (e.g., pigments and water content) using a web interface (Fig. 1), and receive customized simulation results.

2.2 Experimental Sets and Specimen Characterization Data

Usually, the assessment of changes in skin appearance attributes is performed considering nonpalmoplantar areas normally



Run HyLloS Online

www.npsg.uwaterloo.ca/models/hyllos.php

Natural Phenomena Simulation Group
University of Waterloo

Home News Members Research Data Models Guides Gallery Misc. Contact

HyLloS

Hyperspectral Light Impingement on Skin

(Standard Version)

The HyLloS model uses a Monte Carlo formulation to simulate light interaction with human skin. Melanosomes are created and discarded on the fly as the light propagates through the skin tissue. The light rays can be scattered or absorbed by these organelles as well as other skin constituents. For more details about this model, please read our related publication (2015).

Note that HyLloS provides bidirectional readings. However, one can obtain directional-hemispherical quantities (provided by our online system) by integrating the outgoing light (rays) with respect to the collection hemisphere. Similarly, bihemispherical quantities can be calculated by integrating the BDF (bidirectional scattering distribution function) values with respect to incident and collection hemispheres.

The spectral input data files for the materials considered by the online HyLloS model are available [here](#). The full set of model parameters, including those normally not subject to change for the simulations, can be accessed in the [extended version](#) of this website.

Additional Notes

- Usually only the biophysical parameters (on the right) written on **boldface** need to be changed to represent markedly different human skin specimens (e.g., lightly pigmented, heavily pigmented, young and old). The default estimated values assigned to these parameters correspond to a young and lightly pigmented human skin specimen. The default values assigned to the other biophysical parameters correspond to measured and estimated average skin data found in the biomedical literature.
- Some properties are precomputed for optimization. These parameters are presented as combo boxes.

Run HyLloS Online

Enter your email address: (used to send the results)

Model Parameter	Value
Number of samples	<input type="text" value="100000"/>
Angle of incidence	<input type="text" value="8"/> degrees
Wavelength range	<input type="text" value="400-700"/> nm
Aspect ratio of skin surface folds	<input type="text" value="0.1"/>
Stratum corneum thickness	<input type="text" value="0.0004"/> cm
Stratum granulosum thickness	<input type="text" value="0.0033"/> cm
Stratum spinosum thickness	<input type="text" value="0.0033"/> cm
Stratum basale thickness	<input type="text" value="0.0033"/> cm
Papillary dermis thickness	<input type="text" value="0.02"/> cm
Reticular dermis thickness	<input type="text" value="0.125"/> cm
Percentage of stratum granulosum occupied by melanosomes	<input type="text" value="0"/> %
Percentage of stratum spinosum occupied by melanosomes	<input type="text" value="0"/> %
Percentage of stratum basale occupied by melanosomes	<input type="text" value="3"/> %
Percentage of stratum granulosum occupied by volumetric melanin	<input type="text" value="1.35"/> %
Percentage of stratum spinosum occupied by volumetric melanin	<input type="text" value="1.35"/> %
Percentage of stratum basale occupied by volumetric melanin	<input type="text" value="1.35"/> %
Stratum basale melanosome dimensions	<input type="text" value="0.41 um X 0.17 um (light)"/>
Concentration of eumelanin in the melanosomes	<input type="text" value="32.0 g/L"/>
Concentration of pheomelanin in the melanosomes	<input type="text" value="2.0 g/L"/>
Percentage of papillary dermis occupied by blood	<input type="text" value="0.3"/> %
Percentage of reticular dermis occupied by blood	<input type="text" value="0.3"/> %
Percentage of oxygenated hemoglobin	<input type="text" value="75"/> %

Submit

Fig. 1 The web interface for the Hyperspectral Light Impingement on Skin (HyLloS) model²⁵ available through the Natural Phenomena Simulation Group Distributed framework.³⁰ Through this web interface,²⁹ researchers can configure physical parameters and execute light transport simulations involving different skin specimens.

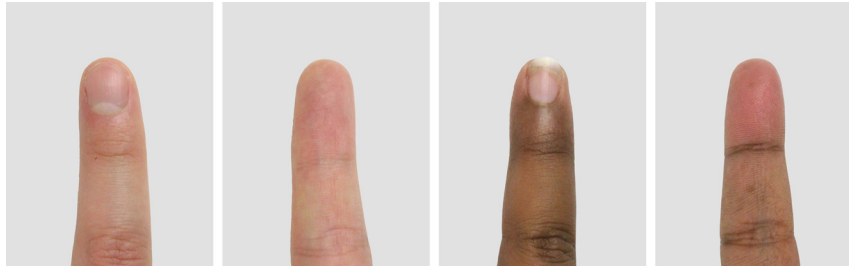


Fig. 2 Photographs depicting the dorsal and palmar surfaces of the index finger (in a position below heart level) of a lightly pigmented (left) and a darkly pigmented (right) subject. The camera was placed above the specimens and the ambient (nondirectional) illumination was provided by fluorescent lamps.

exposed to light, such as the face and the back of the hand. However, the noninvasive measurement of blood-related properties is usually at hypopigmented sites less affected by the presence of melanin, such as the palmar fingertips (Fig. 2). Accordingly, our investigation involved two sets of *in silico* experiments. In the first set, we employed HyLloS to generate directional-hemispherical reflectance curves depicting the spectral effects of reduced Hb concentrations in nonpalmoplantar areas characterized by average pigmentation and morphological parameters, such as the dorsal surface of the fingers. In order to expand our scope of observations, these simulations were performed considering skin specimens with different levels of pigmentation, henceforth referred to as lightly pigmented (LP) and darkly pigmented (DP). These levels of pigmentation are mostly determined by the presence of the main absorbers acting in the visible domain, namely the melanins (in colloidal and aggregated forms) and the functional hemoglobins, whose absorption spectra are depicted in Fig. 3. In the second set, we repeat the simulations for the hypopigmented areas, more specifically the palmar fingertips of the LP and DP specimens. In these simulations, we took into account the particular characteristics of these cutaneous sites, namely the increased epidermal thickness,³¹ the reduced presence of melanin proteins (more than fivefold lower than in nonpalmoplantar epidermis³²), and the increased blood fractional volume³³ (especially when the fingertip is in a position below heart level³⁴).

Both sets of *in silico* experiments were performed with respect to UV, visible, and NIR regions of the light spectrum where skin spectral responses to variations in Hb concentration have a higher probability to be detected, more specifically, in the 250 to 850 nm range.^{25,37} Unless otherwise stated, the resulting reflectance data were obtained considering an angle of incidence of 10 deg. The specific parameters employed in the characterization of the skin tissues considered in the first and second sets of *in silico* experiments are provided in Tables 1 and 2, respectively, while characterization parameters employed in both sets of experiments are provided in Table 3. In order to account for melanosome degradation in the upper epidermal layers,³⁸ the axes of the melanosomes located in the stratum spinosum and stratum granulosum were set to be, respectively, 50 and 25% of the values considered for the melanosomes in the stratum basale of the LP and DP specimens depicted in Tables 1 and 2. We remark that the values assigned to the specific and general parameters listed in Tables 1–3 were selected based on actual biophysical ranges provided in the scientific literature, and their respective reference sources are also included in these tables. Similarly, the reductions in Hb concentration associated with the anemia severity levels considered in this investigation

were also selected according to values provided in the scientific literature as depicted in Tables 4 and 5.

2.3 Sensitivity Measure

In order to assess the spectral variation patterns resulting from our *in silico* experiments more systematically, we performed a differential sensitivity analysis⁷⁹ on the corresponding modeled reflectance curves across selected spectral ranges [UV (250 to

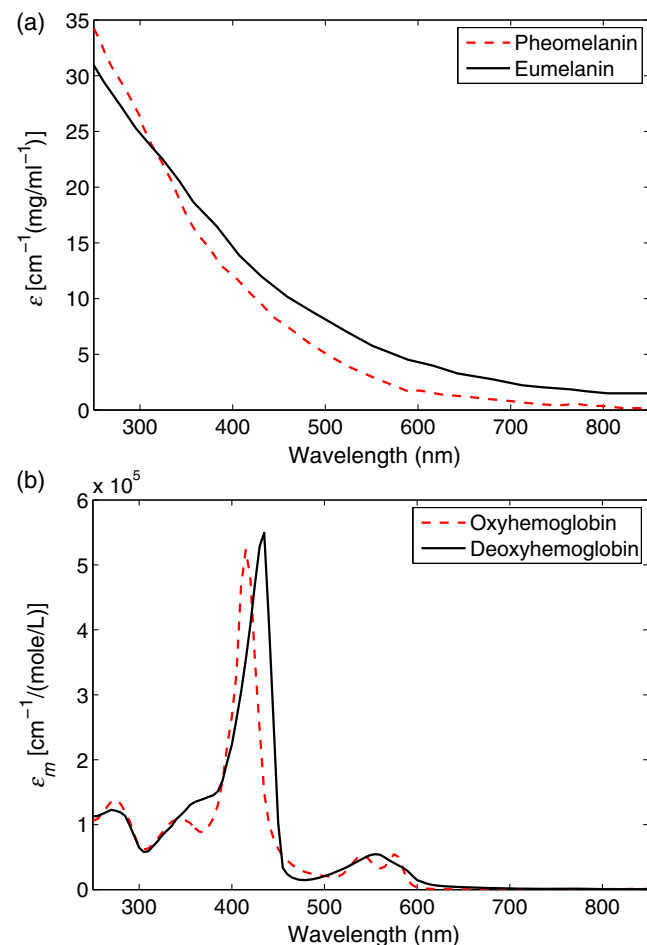


Fig. 3 Absorption spectra of key absorbers found in the skin tissues, namely melanins and functional hemoglobins, whose contents were subjected to variations during this investigation. (a) Extinction coefficient (ϵ) curves for the melanins.³⁵ (b) Molar extinction coefficient (ϵ_m) curves for the functional hemoglobins.³⁶ Note that the contents of keratin, DNA, uranic acid, beta-carotene, bilirubin, disfunctional hemoglobins lipids, and water were also accounted for in this investigation.

Table 1 HyLloS model parameters employed in the characterization of the skin tissues found in the dorsal surface of the fingers belonging to the two specimens, lightly (LP) and darkly (DP) pigmented, considered in this investigation.

Parameter	LP	DP	Source
Stratum corneum thickness (cm)	0.001	0.002	39–42
Stratum granulosum thickness (cm)	0.0046	0.0015	31
Stratum spinosum thickness (cm)	0.0046	0.0015	31
Stratum basale thickness (cm)	0.0046	0.0015	31
Papillary dermis thickness (cm)	0.02	0.023	43
Reticular dermis thickness (cm)	0.125	0.2	43
Stratum granulosum melanosome content (%)	0.0	5.0	44,45
Stratum spinosum melanosome content (%)	0.0	5.0	44,45
Stratum basale melanosome content (%)	1.0	5.0	44,45
Stratum granulosum colloidal melanin content (%)	0.9	5.0	44,46,47
Stratum spinosum colloidal melanin content (%)	0.9	5.0	44,46,47
Stratum basale colloidal melanin content (%)	0.9	5.0	44,46,47
Stratum basale melanosome dimensions ($\mu\text{m} \times \mu\text{m}$)	0.41×0.17	0.69×0.28	26
Melanosome eumelanin concentration (mg/mL)	32.0	50.0	48,49
Melanosome pheomelanin concentration (mg/mL)	2.0	4.0	48,49
Papillary dermis blood content (%)	0.5	0.5	33,50
Reticular dermis blood content (%)	0.2	0.2	33,50

400 nm), Visible-B (400 to 500 nm), Visible-G (500 to 600 nm), Visible-R (600 to 700 nm), and NIR (700 to 850 nm)]. This analysis involves the computation of a sensitivity index that provides the ratio of the change in output to the change in a quantity while the other quantities are kept fixed. A ratio equal to 1.0 indicates complete sensitivity (or maximum impact), while a ratio <0.01 indicates that the output is insensitive to changes in the selected quantity.⁸⁰ Accordingly, we computed the mean sensitivity index (MSI) for the spectral regions of interest to assess the mean ratio of change in reflectance with respect to the change in the selected quantity, namely dermal Hb concentration, associated with the three anemia severity levels (Table 4) under study. This index is expressed as

$$\text{MSI} = \frac{1}{N} \sum_{i=1}^N \frac{|\rho_n(\lambda_i) - \rho_a(\lambda_i)|}{\max\{\rho_n(\lambda_i), \rho_a(\lambda_i)\}}, \quad (1)$$

where ρ_n and ρ_a correspond to the reflectances associated with the nonanemic (baseline) and anemic cases, respectively, computed for a given skin specimen, and N is the total number of wavelengths sampled with a 5-nm resolution within a selected spectral region.

2.4 Skin Swatches

In this investigation, we have also generated skin swatches to demonstrate that the use of visual inspections to detect the

onset of anemia and monitor its progression can be hindered by physiological and technical factors. These swatches were rendered using the modeled reflectance data obtained for the LP and DP specimens using HyLloS, and considering three distinct CIE standard illuminants, whose respective relative spectral power distributions are provided in Fig. 4. The resulting swatch color is obtained from the convolution of the illuminant spectral power distribution spectrum, the modeled skin reflectance data, and the broad spectral response of the human photoreceptors.⁸¹ This last step was performed employing a standard XYZ to sRGB conversion procedure.^{16,82}

3 Results and Discussion

The results of our first set of *in silico* experiments involving the dorsal surface of the fingers of the LP and DP specimens are presented in Fig. 5. As expected, these results show that reductions in Hb concentration associated with increasing anemia severity levels have a more noticeable magnifying effect on the reflectance of the LP specimen. These spectral responses are less affected by the light attenuation properties of melanin (in colloidal and aggregated forms) than its DP specimen's counterpart.

As indicated by the MSI values presented in Fig. 6, the impact of the Hb concentration reduction is markedly stronger in the visible region, particularly in the 500 to 600 nm range, for the LP specimen with respect to three severity levels. This observation can be explained by the fact that although the UV absorption profile of the hemoglobins (O_2Hb and HHb) is high

Table 2 Datasets of specific parameters employed in the characterization of skin tissues found in the palmar fingertip of the two specimens, LP and DP, considered in this investigation.

Parameter	LP	DP	Source
Stratum corneum thickness (cm)	0.013	0.026	39,51,52
Stratum granulosum thickness (cm)	0.0123	0.006	31,52
Stratum spinosum thickness (cm)	0.0123	0.006	31,52
Stratum basale thickness (cm)	0.0123	0.006	31,52
Papillary dermis thickness (cm)	0.02	0.023	43
Reticular dermis thickness (cm)	0.125	0.2	43
Stratum granulosum melanosome content (%)	0.0	0.25	32,44,45
Stratum spinosum melanosome content (%)	0.0	0.25	32,44,45
Stratum basale melanosome content (%)	0.15	0.25	32,44,45
Stratum granulosum colloidal melanin content (%)	0.06	0.25	32,44,47
Stratum spinosum colloidal melanin content (%)	0.06	0.25	32,44,47
Stratum basale colloidal melanin content (%)	0.06	0.25	32,44,47
Stratum basale melanosome dimensions ($\mu\text{m} \times \mu\text{m}$)	0.41×0.17	0.69×0.28	26
Melanosome eumelanin concentration (mg/mL)	32.0	50.0	48,49
Melanosome pheomelanin concentration (mg/mL)	2.0	4.0	48,49
Papillary dermis blood content (%)	5.0	5.0	33,34,50
Reticular dermis blood content (%)	0.5	0.5	33,34,50

(Fig. 3), eumelanin and pheomelanin, albeit in small amounts, have a dominant attenuation role in this spectral region.^{25,37} In the NIR region, on the other hand, not only the Hb absorption profile is relatively low, but light attenuation is also affected by the presence of water and lipids.^{25,37}

For the DP specimen, the impact is minor across all selected spectral regions with respect to the mild and moderate levels. It becomes somewhat significant, notably in the visible-G (500 to 600 nm) range (Fig. 6), only when the anemia condition reaches the severe level. In this case, the substantial reduction of Hb concentration can slightly counterpose the strong light attenuation performed by the relatively large amounts of melanin present in the epidermal tissues. In addition, as further illustrated by the skin swatches depicted in Fig. 7, while one can notice changes in skin colorimetric parameters, namely lightness and hue (toward a pale and a yellowish appearance, respectively), following a reduction in Hb concentration in the LP specimen, such variations, particularly with respect to hue, are not as discernible in the DP specimen.

The results of our second set of *in silico* experiments involving the palmar fingertips of the LP and DP specimens are presented in Fig. 8. They show that reductions in Hb concentration associated with increasing anemia severity levels have noticeable effects on the spectral responses of both pigmented specimens considered in this investigation. We remark that the palmar fingertips are hypopigmented areas³² regardless of the native level of pigmentation of an individual (e.g., Fig. 2)

and are characterized by a higher blood volume content in the dermal tissues.³³ Hence, the spectral responses of these cutaneous sites are less affected by the small presence of melanin proteins. Furthermore, as indicated by the MSI values presented in Fig. 9, the impact of variations in Hb concentration also increases monotonically with the increasing anemia severity levels, and it is markedly stronger in the visible-G (500 to 600 nm) range for both specimens.

Although the effects resulting from reduced Hb concentrations are clearly detectable for both specimens through spectrophotometric measurements, the same degree of detection confidence cannot be obtained through the visual inspection of the specimens' skin appearance attributes. More specifically, as illustrated by the skin swatches depicted in Fig. 10, the same observations reported earlier for the dorsal surface of the finger swatches apply to the palmar fingertip ones, i.e., while we can notice changes in skin lightness and hue following a reduction in Hb concentration in the LP specimen, hue variations are not as discernible in the DP specimen.

The difficulties imposed by different levels of pigmentation on the visual inspection of skin specimens can be exacerbated by other factors, such as the intensity and spectral power distribution of the light sources employed during their screening. For example, as illustrated in the palmar fingertip swatches of the LP specimen presented in Fig. 11, an anemic-like appearance can be elicited by different combinations of these factors. More precisely, although the spectral response used in the generation

Table 3 Dataset of general parameters employed in the characterization of the skin tissues found in the dorsal surface and palmar fingertip of the fingers of both specimens considered in this investigation. The refractive indices for the skin layers were measured at 1300 nm as reported in the listed sources.

Parameter	Value	Source
Surface fold aspect ratio	0.1	53,54
Oxygenated blood fraction (%)	75.0	55
Stratum corneum refractive index	1.55	56,57
Epidermis refractive index	1.4	17,56
Papillary dermis refractive index	1.39	56,58
Reticular dermis refractive index	1.41	56,58
Melanin refractive index	1.7	59
MetHb concentration in whole blood (mg/mL)	1.5	60
CarboxyHb concentration in whole blood (mg/mL)	1.5	61
SulfHb concentration in whole blood (mg/mL)	0.0	62
Whole blood bilirubin concentration (mg/mL)	0.003	63
Stratum corneum beta-carotene concentration (mg/mL)	$2.1E-4$	64
Epidermis beta-carotene concentration (mg/mL)	$2.1E-4$	64
Blood beta-carotene concentration (mg/mL)	$7.0E-5$	64
Stratum corneum water content (%)	35.0	65,66
Epidermis water content (%)	60.0	65,67
Papillary dermis water content (%)	75.0	65,67
Reticular dermis water content (%)	75.0	65,67
Stratum corneum lipid content (%)	20.0	68
Epidermis lipid content (%)	15.1	65,69,70
Papillary dermis lipid content (%)	17.33	65,69,70
Reticular dermis lipid content (%)	17.33	65,69,70
Stratum corneum keratin content (%)	65.0	71–73
Stratum corneum urocanic acid density (mol/L)	0.01	74
Skin DNA density (mg/mL)	0.185	65,75,76

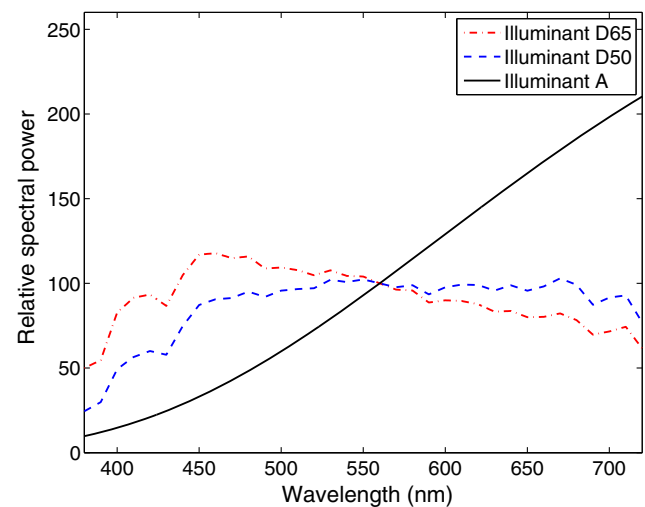
of these swatches corresponds to the nonanemic (baseline) case, some of them have appearance attributes similar to those of the swatches associated with different anemia severity levels presented in Fig. 10, which may lead to misinterpretations of an individual's actual health status. The possibility of occurrence

Table 4 Anemia severity levels for adult individuals (15 years of age and above). The corresponding reductions in hemoglobin (Hb) concentration considered in this investigation were selected according to values provided in the literature.^{1,77,78}

Severity level	Hb reduction (%)	Hb concentration (g/L)
Baseline	—	147.0
Mild	20	117.6
Moderate	40	88.2
Severe	60	58.8

Table 5 Anemia severity levels for children (below 15 years of age) and pregnant women. The corresponding reductions in hemoglobin (Hb) concentration considered in this investigation were selected according to values provided in the literature.^{1,77,78}

Severity level	Hb reduction (%)	Hb concentration (g/L)
Baseline	—	125.0
Mild	20	100.0
Moderate	40	75.0
Severe	60	50.0

**Fig. 4** Relative spectral power distributions of three CIE standard illuminants, namely D65, D50, and A, considered in our investigation. While the first two correspond to average daylight with correlated color temperatures of 6504 and 5503 K, respectively, the third one corresponds to a gas-filled tungsten lamp operating at a correlated color temperature of 2856 K.^{19,83}

of such situations, which are usually associated with metamerism problems,^{18,83} can also be verified when we compare some of the nonanemic swatches of the DP specimen presented in Fig. 12 with the anemic swatches presented in Fig. 10 for this specimen. Similarly, as illustrated in Figs. 13 and 14, the intensity and the spectral power distribution of the light sources can also affect subjective quantifications of anemia severity levels

based on expected appearance attributes, such as paleness and yellowness.

Several symptoms (e.g., tiredness and faintness) and signs (e.g., pale or yellowish skin mentioned earlier) provide clues to physicians about the possible onset of anemia in a patient.⁴ In order to verify this possibility and deliver a diagnosis with a higher degree of certainty, physicians usually require a blood exam. This is used to determine, among other factors, whether the patient's Hb concentration is below the level considered normal for people within the same age group and with similar physiological characteristics. Once it has been established that the patient is anemic and the recommended treatment starts, the condition should be monitored to evaluate whether the patient's Hb concentration is returning to the normal level. Again, clinical assessment procedures, such as visual inspections and blood exams, can be employed.⁴ We remark, however, that while the former may lead to incorrect interpretations as illustrated before, the latter may not be readily available at the point-of-care on a regular basis.

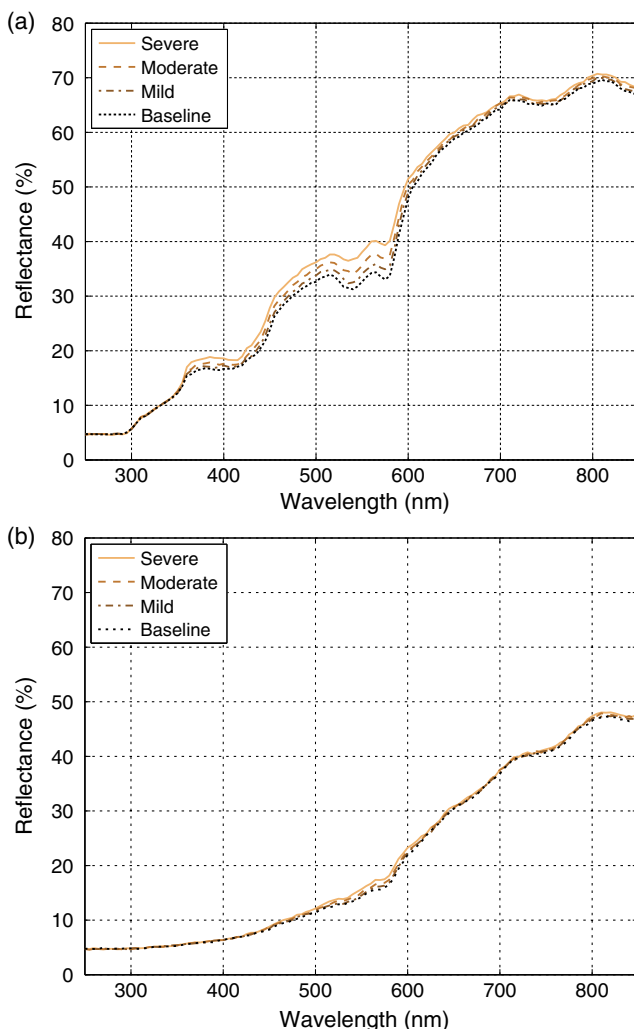


Fig. 5 Modeled skin reflectance curves for the dorsal surface of the fingers of the (a) lightly and (b) darkly pigmented specimen showing the spectral responses elicited by distinct dermal Hb concentrations associated with increasing anemia severity levels, namely baseline (nonanemic level, 147.0 g/L), mild (117.6 g/L), moderate (88.2 g/L), and severe (58.8 g/L). The modeled curves were obtained considering the data provided in Tables 1, 3, and 4.

The results of our second set of *in silico* experiments suggest that the monitoring of anemia can be assisted by an index, henceforth referred to as the anemia monitoring index (AMI), which can be obtained through a noninvasive spectrophotometric measurement performed at the patient's palmar fingertip. As depicted in Figs. 8 and 9, variations in Hb concentration have a detectable impact on the palmar fingertip reflectance of specimens with distinct levels of native skin pigmentation, more prominently in the Visible-G spectral region. Moreover, this impact is uniform in this region, i.e., as the Hb concentration decreases, the reflectance increases across the entire 500 to 600 nm range. This suggests that a single sample wavelength within this range can be used to monitor these variations. Considering that the monitoring of an anemic patient may need to take place within an extended period of time, it is necessary to mitigate the chances of its results being affected by other physiologic factors.

In order to address this issue, a number of guidelines should be used in the selection of a suitable monitoring point. First,

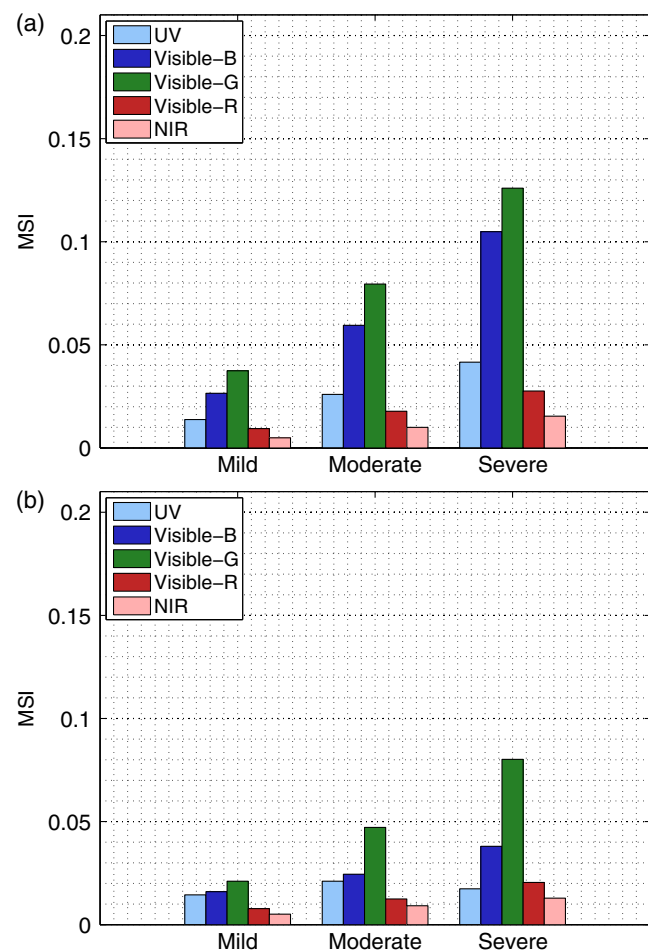


Fig. 6 Mean sensitivity index (MSI) values computed for the modeled anemic skin reflectance curves (mild, moderate, and severe) obtained for the dorsal surface of the fingers of the (a) lightly and (b) darkly pigmented specimen (Fig. 5). The MSI values were computed for each anemic skin reflectance curve [across selected UV (250 to 400 nm), Visible-B (400 to 500 nm), Visible-G (500 to 600 nm), Visible-R (600 to 700 nm), and near-infrared (NIR) (700 to 850 nm) ranges] with respect to the baseline curve (nonanemic level) associated with the respective specimen.

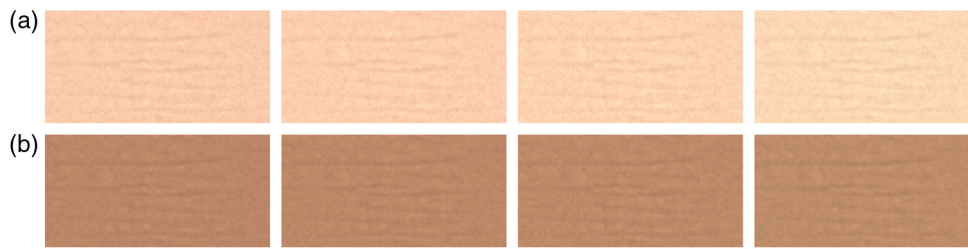


Fig. 7 Skin swatches depicting tone variations on the dorsal surface of the fingers of the (a) lightly and (b) darkly pigmented specimens. These variations, which were obtained by reducing the dermal Hb concentration (from left to right, 147.0, 117.6, 88.2, and 58.8 g/L), illustrate the visual effects of increasing anemia severity levels, namely baseline (nonanemic level), mild, moderate, and severe, respectively (Table 4). The swatches were rendered considering a D50 illuminant (Fig. 4) and using the corresponding skin spectral responses provided by the HyLloS model (Fig. 5).

it should be a wavelength at which O_2Hb and HHb have the same extinction coefficient values (isosbestic point⁸⁴) to avoid influences from changes in the blood oxygenation levels. We note that there are several isosbestic points (500, 530, 545, 570, and 584 nm⁸⁵) in the spectral region of interest (Fig. 3). Second, it should be located away from the spectral region where water and lipids have a strong impact on light absorption^{25,37} to avoid masking effects, for example, from transepidermal water loss.⁸⁶ Third, it should also be located away from the absorption spectra of other chromophores associated with the onset of medical conditions with similar effects on a patient's visual appearance attributes. As a characteristic example of the latter, one can mention bilirubin,⁸⁷ whose excess in the blood stream is associated with hyperbilirubinemia, or jaundice, which can also result in possible variations in skin appearance attributes (e.g., yellowness) of a patient. Taking these guidelines into consideration, two isosbestic wavelengths, namely 545 and 570 nm, emerge as the most suitable candidates for the monitoring point. It is also necessary to consider that even though the presence of melanin proteins in the palmar fingertip epidermis is fairly low, it cannot be completely discarded.³² Hence, since the corresponding extinction coefficient values for the melanins are lower at 570 nm than at 545 nm (Fig. 3), we selected the former.

A relatively simple anemia monitoring procedure could then be employed using a single reflectance measurement at 570 nm. Preferably, the patient's finger should be in a position below heart level to maximize the blood fractional volume,³⁴ with the patient's forearm resting passively to minimize shear rate fluctuations on the blood flow that could affect its optical properties.⁸⁸ Moreover, since this measurement might need to be repeated a number of times during the treatment, it would be advisable to select a specific measurement site (e.g., at the center of the tactile elevations) for consistency. Although the adoption of this protocol would contribute to making the procedure more effective, one may still need to account for the possibility of small changes in the measurement conditions. For example, one can expect small angular variations with respect to the angle of incidence due to slight curvature of the palmar fingertip. In order to examine the robustness of the proposed procedure with respect to such fluctuations, we computed the reflectance at 570 nm for the LP and DP specimens considering three angles of incidence, namely 0, 10 (the default value employed in our *in silico* experiments), and 20 deg. Furthermore, since the anemia severity levels may vary with age and, in the case of female patients, pregnancy,¹ we performed these computations with respect to a broader scope of Hb concentrations by including all values depicted in Tables 4 and 5.

As expected, the resulting reflectance values presented in Table 6 for all three angles of incidence depict a vertical increase with respect to Hb concentration reduction, which becomes more prominent as the condition worsens. Moreover, for each

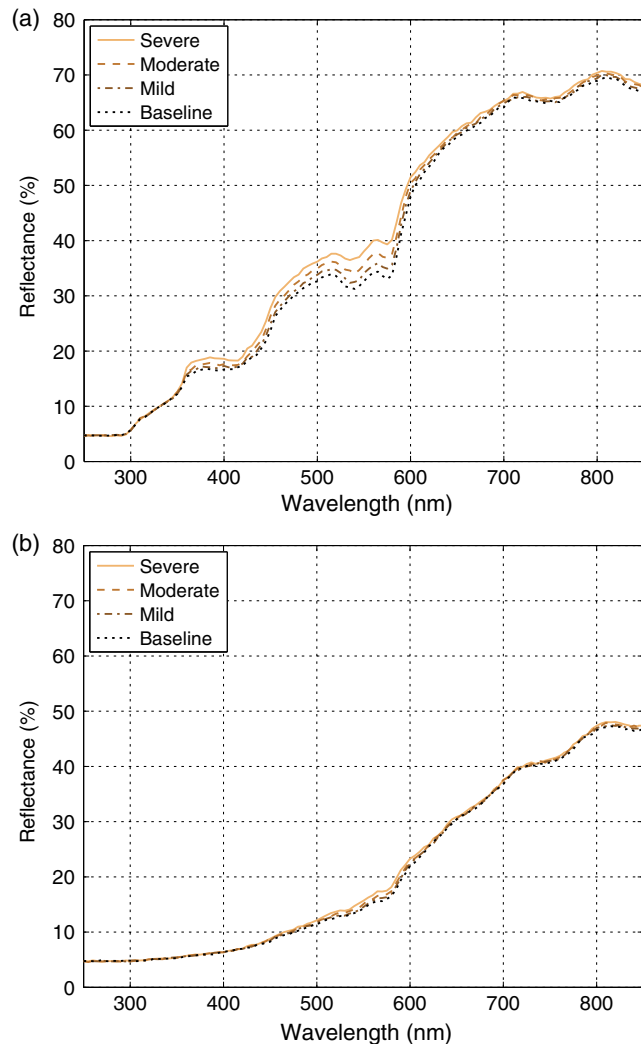


Fig. 8 Modeled skin reflectance curves for the palmar fingertips of the (a) lightly and (b) darkly pigmented specimen showing the spectral responses elicited by distinct dermal Hb concentrations associated with increasing anemia severity levels, namely baseline (nonanemic level, 147.0 g/L), mild (117.6 g/L), moderate (88.2 g/L), and severe (58.8 g/L). The modeled curves were obtained considering the data provided in Tables 2, 3, and 4.

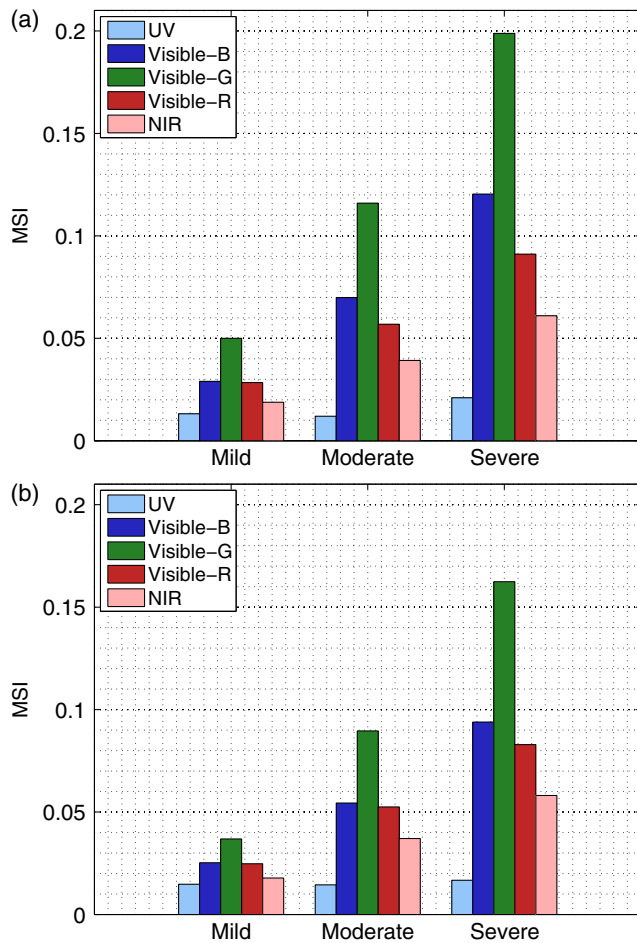


Fig. 9 MSI values computed for the modeled anemic skin reflectance curves (mild, moderate, and severe) obtained for the palmar fingertips of the (a) lightly and (b) darkly pigmented specimens (Fig. 8). The MSI values were computed for each anemic skin reflectance curve [across selected UV (250 to 400 nm), Visible-B (400 to 500 nm), Visible-G (500 to 600 nm), Visible-R (600 to 700 nm), and NIR (700 to 850 nm) ranges] with respect to the baseline curve (nonanemic level) associated with the respective specimen.

specific Hb concentration value, they also show a slight horizontal decrease with respect to the angle of incidence. In some instances, however, the same value was recorded for two angles of incidence. This can be attributed to the stochastic nature of our simulations. More importantly, the observed horizontal reflectance variations with the angle of incidence are smaller

than the vertical reflectance variations associated with significant changes in the Hb concentration.

It is worth noting that even well-designed and carefully calibrated spectrophotometers can yield results from the same specimen that differ from one measurement to the next.^{16,89} These differences, or uncertainties, are caused by variations in the components of the instrument, fluctuations in environmental conditions, and changes in the specimen handling procedure. A spectrophotometer is considered to be of high precision if the spectral measurements have an uncertainty of $\sim \pm 0.001$.^{89,90} Hence, the horizontal reflectance variations depicted in our simulations have a magnitude comparable to the uncertainty of actual spectral measurements.

In summary, our findings suggest that once the onset of anemia has been established, this blood disorder can be reliably monitored using a relatively simple procedure. At the time of the onset confirmation, the patient's AMI would be measured and recorded. Afterward, during the treatment, the patient's anemic level could be monitored by performing subsequent AMI measurements and comparing their values with previously recorded ones. Clearly, a more accurate assessment can be obtained through blood exams performed using traditional laboratory procedures. However, considering that the proposed AMI would be obtained through a reflectance measurement performed at a single wavelength, we believe that it would require a simpler and more cost-effective device than a standard spectrophotometer, making its use attractive for low-resources diagnosis settings with limited access to laboratory facilities. We also remark that such a measurement would be noninvasive and performed at a wavelength within the visible (nonharmful) region of the light spectrum.

4 Conclusion

Arguably, anemia is among the most widespread blood disorders that can lead to serious health impairment and, if not properly treated, fatal situations. Not surprisingly, the physiological changes associated with this condition, particularly the reduction of Hb concentration, have been the object of extensive research aimed at their quantification and interpretation. The biomedical procedures employed in these tasks vary from a simple visual inspection of a patient's appearance to a wide range of laboratory exams of blood samples. With the recent advances in optics and photonics, a wide range of invasive and noninvasive devices are being proposed to assist these tasks. In the latter case, the reliability of the results depends on the correct assessment of the skin spectral responses to these changes. However, the *in vivo* investigation of these responses is often hindered by



Fig. 10 Skin swatches depicting tone variations on the palmar fingertips of the (a) lightly and (b) darkly pigmented specimens. These variations, which were obtained by reducing the dermal Hb concentration (from left to right, 147.0, 117.6, 88.2, and 58.8 g/L), illustrate the visual effects of increasing anemia severity levels, namely baseline (nonanemic level), mild, moderate, and severe, respectively (Table 4). The swatches were rendered considering a D50 illuminant (Fig. 4) and using the corresponding skin spectral responses provided by the HyLloS model (Fig. 8).



Fig. 11 Skin swatches illustrating tone variations on the fingertip of the lightly pigmented specimen (with a baseline Hb concentration equal to 147.0 g/L) resulting from employing distinct light sources (Fig. 4), namely (a) D65, (b) D50, and (c) A, whose default intensity value (left column) was increased by 15% (middle column) and 30% (right column). The swatches were rendered using skin spectral responses provided by the HyLloS model,²⁵ which, in turn, were obtained using the data provided in Tables 2 and 3.



Fig. 12 Skin swatches illustrating tone variations on the fingertip of the darkly pigmented specimen (with a baseline Hb concentration equal to 147.0 g/L) resulting from employing distinct light sources (Fig. 4), namely (a) D65, (b) D50, and (c) A, whose default intensity value (left column) was increased by 15% (middle column) and 30% (right column). The swatches were rendered using skin spectral responses provided by the HyLloS model,²⁵ which, in turn, were obtained using the data provided in Tables 2 and 3.



Fig. 13 Skin swatches illustrating tone variations on the fingertip of the lightly pigmented specimen (with a baseline Hb concentration equal to 58.0 g/L) resulting from employing distinct light sources (Fig. 4), namely (a) D65, (b) D50, and (c) A, whose default intensity value (left column) was increased by 15% (middle column) and 30% (right column). The swatches were rendered using skin spectral responses provided by the HyLloS model,²⁵ which, in turn, were obtained using the data provided in Tables 2 and 3.



Fig. 14 Skin swatches illustrating tone variations on the fingertip of the darkly pigmented specimen (with a baseline Hb concentration equal to 58.0 g/L) resulting from employing distinct light sources (Fig. 4), namely (a) D65, (b) D50, and (c) A, whose default intensity value (left column) was increased by 15% (middle column) and 30% (right column). The swatches were rendered using skin spectral responses provided by the HyLloS model,²⁵ which, in turn, were obtained using the data provided in Tables 2 and 3.

Table 6 Reflectance values at 570 nm computed for the palmar fingertip of the LP and DP specimens considering distinct hemoglobin (Hb) concentrations and three angles of incidence, namely 0 deg, 10 deg (the default value used in this investigation), and 20 deg. Each reflectance value was computed using 10^6 sample rays and depicted using a four-digit chopping arithmetic.

Hb concentration (g/L)	LP			DP		
	0 deg	10 deg	20 deg	0 deg	10 deg	20 deg
147.0	0.291	0.290	0.289	0.241	0.241	0.241
125.0	0.301	0.301	0.299	0.248	0.247	0.247
117.6	0.307	0.306	0.303	0.250	0.250	0.249
100.0	0.319	0.318	0.316	0.259	0.258	0.257
88.2	0.329	0.328	0.326	0.265	0.265	0.264
75.0	0.342	0.341	0.341	0.275	0.274	0.273
58.8	0.365	0.365	0.362	0.289	0.289	0.288
50.0	0.381	0.380	0.379	0.300	0.300	0.299

practical difficulties, such as the control of a large number of biophysical variables.

In this paper, we employed a first principles light transport model of light and skin interactions to examine these responses with respect to different spectral, observational, and physiological conditions. The results of our controlled *in silico* experiments demonstrate that the influence of melanin pigmentation on the effective detection of these responses can be substantially mitigated by selecting a cutaneous site, such as the palmar fingertip, with suitable characteristics, namely hypopigmentation and increased dermal blood content. Furthermore, our findings also indicate that significant variations in the anemia severity levels associated with Hb concentration reductions can be monitored by measuring the patient's skin reflectance at a selected spectral sampling point (570 nm) affected neither by blood oxygenation variations nor by changes in the presence of other relevant absorbers (e.g., bilirubin and water) in the skin tissues. Based on these observations, we proposed the use of such

reflectance (AMI) measurements as the integral component of a procedure to assist the monitoring of anemic patients in regions not served by comprehensive health care resources on a regular basis.

As future work, we intend to address the actual implementation of the proposed anemia monitoring procedure. Accordingly, we plan to investigate the feasibility of different alternatives for performing the AMI measurements at the point-of-care. These include the enhancement of existing devices to incorporate AMI measurements and the design of a new portable instrument specifically dedicated to providing this index with a high accuracy to cost ratio.

Acknowledgments

This work was partially supported by the Natural Sciences and Research Council of Canada (NSERC) under NSERC Grant 238337.

References

- World Health Organization, *VMNIS - Vitamin and Mineral Nutrition Information System*, pp. 1–6, Geneva, Switzerland 2011 <http://www.who.int/vmnis/indicators/haemoglobin.pdf> (30 Jul 2015).
- E. McLean et al., "Worldwide prevalence of anaemia, WHO Vitamin and Mineral Nutrition System, 1993–2005," *Public Health Nutr.* **12**(3), 444–454 (2003).
- B. de Benoist et al., Eds., *Worldwide prevalence of anaemia 1993–2005 who global database on anaemia*, World Health Organization, Geneva, Switzerland (2001).
- U.S. Department of Health and Human Services, "Your guide to anemia," Technical Report NIH 11-7629, National Institutes of Health, National Heart, Lung and Blood Institute, Bethesda, MD (2011).
- G. V. G. Baranoski et al., "On the noninvasive optical monitoring and differentiation of methemoglobinemia and sulfhemoglobinemia," *J. Biomed. Opt.* **17**(9), 097005 (2012).
- A. Maton et al., *Human Biology and Health*, Prentice Hall, Englewood Cliffs, New Jersey (1993).
- H. Schenck, M. Falkensson, and B. Lundberg, "Evaluation of 'HemoCue', a new device for determining hemoglobin," *Clin. Chem.* **32**(3), 526–529 (1986).
- M. Bond et al., "Chromatography paper as a low-cost medium for accurate spectrophotometric assessment of blood hemoglobin concentration," *Lab Chip* **13**, 2381–2388 (2013).
- L. Lamhaut et al., "Comparison of the accuracy of noninvasive hemoglobin monitoring by spectrophotometry (SpHb) and HemoCue with automated laboratory hemoglobin measurement," *Anesthesiology* **115**(3), 548–554 (2011).
- M. Bond et al., "Design and performance of a low-cost, handheld reader for diagnosing anemia in Blantyre, Malawi," in *Health Innovations and Point-of-Care Technologies Conf.*, pp. 267–270 (2014).
- C. Crowley et al., "Validity and correspondence of non-invasively determined hemoglobin concentrations by two trans-cutaneous digital measuring devices," *Asia Pacific J. Clin. Nutr.* **21**, 191–200 (2012).
- R. Doshi and A. Panditrao, "Non-invasive optical sensor for hemoglobin determination," *Int. J. Eng. Res. Appl.* **3**, 559–562 (2013).
- J. Kraitl et al., "Non-invasive measurement of blood components. Sensors for an in-vivo hemoglobin measurement," in *Advancement in Sensing Technology: New Developments and Practical Applications*, S. C. Mukhopadhyay, K. P. Jayasundera, and A. Fuchs, Eds., pp. 237–262, Springer, Berlin, Germany (2013).
- P. Zakharov, M. S. Talary, and A. Caduff, "A wearable diffuse reflectance sensor for continuous monitoring of cutaneous blood content," *Phys. Med. Biol.* **54**, 5301 (2009).
- S. Watanabe et al., "Measuring hemoglobin amount and oxygen saturation of skin with advancing age," *Proc. SPIE* **8229**, 822905 (2012).
- G. V. G. Baranoski and A. Krishnaswamy, *Light & Skin Interactions: Simulations for Computer Graphics Applications*, Morgan Kaufmann/Elsevier, Burlington, Massachusetts (2010).
- V. Tuchin, *Tissue Optics: Light Scattering Methods and Instruments for Medical Diagnosis*, SPIE Press, Bellingham, WA (2007).
- R. Hunter and R. Harold, *The Measurement of Appearance*, 2nd ed., John Wiley & Sons, New York (1987).
- N. Ohta and A. Robertson, *Colorimetry Fundamentals and Applications*, John Wiley & Sons, New York (1982).
- A. Yoshida et al., "Assessment of noninvasive, percutaneous hemoglobin measurement in pregnant and early postpartum women," *Med. Dev.* **7**, 11–16 (2014).
- L. Wang, S. Jacques, and L. Zheng, "MCML–Monte Carlo modelling of light transport in multi-layered tissues," *Comput. Methods Programs Biomed.* **47**, 131–146 (1995).
- G. Baranoski, T. Chen, and A. Krishnaswamy, "Multilayer modeling of skin color and translucency," in *Computational Biosphysics of the Skin*, B. Querleux, Ed., pp. 3–24, Pan Stanford Publishing, Singapore (2014).
- I. Meglinski et al., "Dermal component-based optical modeling of skin translucency: impact on skin color," in *Computational Biosphysics of the Skin*, B. Querleux, Ed., pp. 25–62, Pan Stanford Publishing, Singapore (2014).
- B. Ventura et al., "From in vivo to in silico biology and back," *Nat. Biotechnol.* **443**, 527–553 (2006).
- T. Chen et al., "Hyperspectral modeling of skin appearance," *ACM Trans. Graph.* **34**(3), 1–14 (2015).
- R. L. Olson, J. Gaylor, and M. A. Everett, "Skin color, melanin, and erythema," *Arch. Dermatol.* **108**(4), 541–544 (1973).
- A. Krishnaswamy, G. Baranoski, and J. G. Rokne, "Improving the reliability/cost ratio of goniophotometric measurements," *J. Graph. Tools* **9**(3), 1–20 (2004).
- G. Baranoski, J. Rokne, and G. Xu, "Virtual spectrophotometric measurements for biologically and physically-based rendering," *Vis. Comput.* **17**(8), 506–518 (2001).
- Natural Phenomena Simulation Group (NPSG), *Run HyLioS Online*, School of Computer Science, University of Waterloo, Ontario, Canada, <http://www.npsg.uwaterloo.ca/models/hylioss.php> (2014).
- G. Baranoski et al., "Rapid dissemination of light transport models on the web," *IEEE Comput. Graph. Appl.* **32**, 10–15 (2012).
- J. Whitton and J. Everett, "The thickness of the epidermis," *Br. J. Dermatol.* **89**, 467–476 (1973).
- Y. Yamaguchi et al., "Mesenchymal-epithelial interactions in the skin: increased expression of dickkopf1 by palmo-plantar fibroblast inhibits melanocyte growth and differentiation," *J. Cell Biol.* **165**(2), 275–285 (2004).
- W. Cui, L. Ostrander, and B. Lee, "In vivo reflectance of blood and tissue as a function of light wavelength," *IEEE Trans. Biomed. Eng.* **37**(6), 632–639 (1990).
- R. Turner, G. Burch, and W. Sodeman, "Studies in the physiology of blood vessels in man. III. Some effects of raising and lowering the arm upon the pulse volume and blood volume of the human finger tip in health and in certain diseases of the blood vessels," *J. Clin. Invest.* **16**(5), 789–798 (1937).
- S. L. Jacques, "Optical absorption of melanin," Technical Report, Oregon Medical Laser Center, Portland, OR (2001).
- S. A. Prahl, "Optical absorption of hemoglobin," Technical Report, Oregon Medical Laser Center, Portland, OR (1999).
- R. Anderson and J. Parrish, "Optical properties of human skin," in *The Science of Photomedicine*, J. Regan and J. Parrish, Eds., pp. 147–194, Plenum Press, New York (1982).
- K. P. Nielsen et al., "The importance of the depth distribution of melanin in skin for DNA protection and other photobiological processes," *J. Photochem. Photobiol. B* **82**(3), 194–198 (2006).
- P. Agache, "Stratum corneum histophysiology," in *Measuring the Skin*, P. Agache and P. Humbert, Eds., pp. 95–100, Springer-Berlag, Berlin, Germany (2004).
- P. Agache, "Metrology of the stratum corneum," in *Measuring the Skin*, P. Agache and P. Humbert, Eds., pp. 101–111, Springer-Berlag, Berlin, Germany (2004).
- G. Plewig et al., "Thickness of the corneocytes," in *Stratum Corneum*, R. Marks and G. Plewig, Eds., pp. 171–174, Springer-Verlag, Berlin (1983).
- K. Robertson and J. Rees, "Variation in epidermal morphology in human skin at different body sites as measured by reflectance confocal microscopy," *Acta Derm. Venereol.* **90**, 368–373 (2010).
- R. Anderson and J. Parrish, "The optics of human skin," *Invest. Dermatol.* **77**(1), 13–19 (1981).
- N. Kollias et al., "Photoprotection by melanin," *J. Photochem. Photobiol. B* **9**(2), 135–160 (1991).
- T. S. Lister, *Simulating the color of port wine stain skin*, PhD Thesis, (University of Southampton, United Kingdom 2013).
- S. Alaluf et al., "Ethnic variation in melanin content and composition in photoexposed and photoprotected human skin," *Pigment Cell Res.* **15**, 112–118 (2002).
- M. Pathak, "Functions of melanin and protection by melanin," in *Melanin: Its Role in Human Photoprotection*, M. C. L. Zeise and T. Fitzpatrick, Eds., pp. 125–134, Valdenmar Publishing Co., Overland Park, Kansas (1995).
- A. J. Thody et al., "Pheomelanin as well as eumelanin is present in human epidermis," *J. Invest. Dermatol.* **97**, 340–344 (1991).
- A. Hennessy et al., "Eumelanin and pheomelanin concentrations in human epidermis before and after UVB irradiation," *Pigment Cell Res.* **18**, 220–223 (2005).
- S. L. Jacques, "Origins of tissue optical properties in the UVA, visible, and NIR regions," *OSA TOPS Adv. Opt. Imaging Photon Migr.* **2**, 364–369 (1996).

51. H. Fruhstorfer et al., "Thickness of the stratum corneum of the volar fingertips," *Clin. Anat.* **13**, 429–433 (2000).
52. B. Querleux, L. Darrasse, and J. Bittoun, "Magnetic resonance imaging of human skin in vivo," in *Bioengineering of the Skin Imaging and Analysis*, K. Wilhelm et al., Eds., pp. 99–109, CRC Press, Boca Raton, Florida (2007).
53. P. S. Talreja et al., "Visualization of the lipid barrier and measurement of lipid pathlength in human stratum corneum," *AAPS PharmSci.* **3**(2), 48–56 (2001).
54. N. Magnenat-Thalmann et al., "A computational skin model: fold and wrinkle formation," *IEEE Trans. Inf. Technol. Biomed.* **6**(4), 317–323 (2002).
55. E. Angelopoulou, "Understanding the color of human skin," *Proc. SPIE* **4299**, 243–251 (2001).
56. G. J. Tearney et al., "Determination of the refractive index of highly scattering human tissue by optical coherence tomography," *Opt. Lett.* **20**, 2258–2260 (1995).
57. B. Diffey, "A mathematical model for ultraviolet optics in skin," *Phys. Med. Biol.* **28**(6), 647–657 (1983).
58. S. L. Jacques, C. A. Alter, and S. A. Prahl, "Angular dependence of HeNe laser light scattering by human dermis," *Lasers Life Sci.* **1**, 309–333 (1987).
59. A. N. Bashkatov et al., "Optical properties of melanin in the skin and skin-like phantoms," *Proc. SPIE* **4162**(1), 219–226 (2000).
60. C. E. S. Haymond, R. Cariappa, and M. Scott, "Laboratory assessment of oxygenation in methemoglobinemia," *Clin. Chem.* **51**(2), 434–444 (2005).
61. A. J. Cunningham et al., "Carboxyhemoglobin levels in Kenyan children with plasmodium falciparum malaria," *Am. J. Trop. Med. Hyg.* **71**(1), 43–47 (2004).
62. I. H. Yarynovska and A. Bilyi, "Absorption spectra of sulfhemoglobin derivatives of human blood," *Proc. SPIE* **6094**, 60940G (2006).
63. S. Zucker, P. Horn, and K. Sherman, "Serum bilirubin levels in the US population: gender effect and inverse correlation with colorectal cancer," *Hepatology* **40**, 827–835 (2004).
64. R. Lee et al., "The detection of carotenoid pigments in human skin," *J. Invest. Dermatol.* **64**(3), 175–177 (1975).
65. P. Agache, "Main skin biological constants," in *Measuring the Skin*, P. Agache and P. Humbert, Eds., pp. 727–746, Springer-Berlag, Berlin, Germany (2004).
66. N. Nakagawa, M. Matsumoto, and S. Sakai, "In vivo measurement of the water content in the dermis by confocal Raman spectroscopy," *Skin Res. Technol.* **16**(2), 137–141 (2010).
67. J. A. Viator et al., "A comparative study of photoacoustic and reflectance methods for determination of epidermal melanin content," *J. Invest. Dermatol.* **122**, 1432–1439 (2004).
68. M. L. Williams, M. Hincenbergs, and K. A. Holbrook, "Skin lipid content during early fetal development," *J. Invest. Dermatol.* **91**, 263–268 (1988).
69. C. A. Squier, P. Cox, and P. W. Wertz, "Lipid content and water permeability of skin and oral mucosa," *J. Invest. Dermatol.* **96**(1), 123–126 (1991).
70. A. E. Cerussi et al., "Sources of absorption and scattering contrast for near-infrared optical mammography," *Acad. Radiol.* **8**, 211–218 (2001).
71. E. Fuchs, "Keratins and the skin," *Annu. Rev. Cell Dev. Biol.* **11**(1), 123–154 (1995).
72. H. Shimizu, *Shimizu's Textbook of Dermatology*, Hokkaido University Press, Palo Alto, CA (2007).
73. D. J. Gawkrödger and M. Ardern-Jones, *Dermatology: An Illustrated Colour Text*, 3rd Ed., Churchill Livingstone, Elsevier, New York, NY (2002).
74. A. R. Young, "Chromophores in human skin," *Phys. Med. Biol.* **42**(5), 789 (1997).
75. J. S. Varcoe, *Clinical Biochemistry: Techniques and Instrumentation: A Practical Course*, World Scientific, Singapore (2001).
76. R. Flindt, *Amazing Numbers in Biology*, Springer-Verlag, Berlin, Germany (2006).
77. A. T. Lovell et al., "Determination of the transport scattering coefficient of red blood cells," *Proc. SPIE* **3597**, 175–182 (1999).
78. R. Flewelling, "Noninvasive optical monitoring," in *The Biomedical Engineering Handbook*, 2nd ed., J. D. Bronzino, Ed., 1346–1356, CRC Press LLC, Boca Raton, FL (2000).
79. D. Hamby, "A review of techniques for parameter sensitivity analysis of environmental models," *Environ. Monit. Assess.* **32**, 135–154 (1994).
80. F. Hoffman and R. Gardner, "Evaluation of uncertainties in radiological assessment models," in *Radiological Assessment: A Textbook on Environmental Dose Analysis*, J. Till and H. Meyer, Eds., pp. 1–55, U.S. Nuclear Regulatory Commission, Washington, DC (1983).
81. J. Hopfield, "Olfaction and color vision: more in simpler," in *More is Different: Fifty Years of Condensed Matter Physics*, N. Ong and R. Bhatt, Eds., pp. 269–284, Princeton University Press, Princeton, New Jersey (2001).
82. M. Stone, *A Field Guide to Digital Color*, AK Peters, Natick, Massachusetts (2003).
83. R. W. G. Hunt, *Measuring Colour*, 2nd ed., Ellis Horwood Limited, Chichester, England (1991).
84. H. Zhang, K. Maslov, and L. Wang, "Dark-field confocal photoacoustic microscopy," in *Photoacoustic Imaging and Spectroscopy*, L. V. Wang, Ed., pp. 267–280, CRC Press, Boca Raton, FL (2009).
85. S. Hu and L. V. Wang, "Photoacoustic imaging and characterization of microvasculature," *J. Biomed. Opt.* **15**(1), 011101 (2010).
86. I. Blank, "Factors which influence the water content of the stratum corneum," *J. Invest. Dermatol.* **18**, 433–440 (1952).
87. S. A. Prahl, "Bilirubin," Technical Report, Oregon Medical Laser Center, Portland, OR (2001).
88. D. Yim et al., "A cell-based light interaction model for human blood," *Comput. Graph. Forum* **31**(2), 845–854 (2012).
89. D. Judd and G. Wyszecki, *Color in Business, Science and Industry*, 3rd ed., John Wiley & Sons, New York (1975).
90. D. MacAdam, *Color Measurements Theme and Variations*, Springer Verlag, Berlin, Germany (1981).

Gladimir V. G. Baranoski received his PhD in computer science from the University Calgary, Canada, in 1998. Currently, he is a faculty member of the David R. Cheriton School of Computer Science and the leader of the Natural Phenomena Simulation Group at the University of Waterloo, Canada. His research interests include the predictive simulation of light interactions with natural materials, aiming at interdisciplinary applications involving computer graphics, biomedical optics, and remote sensing.

Ankita Dey received her M.Math. degree in computer science from the University of Waterloo, Canada, in 2015. Her work can be defined as experimental research residing between disciplines: computer science and biology. She is also a member of the Natural Phenomena Simulation Group, David R. Cheriton School of Computer Science at the University of Waterloo. Her research interests lie in the field of biomedical optics, specifically concerning light interactions with human skin.

Tenn F. Chen received his bachelor's and master's degrees in computer science from the University of Waterloo, Canada, in 2006 and 2009, respectively. He is currently pursuing the doctoral degree at the Natural Phenomena Simulation Group, University of Waterloo. His research interests include the predictive simulation of how light interacts with organic and inorganic materials.